Line shape theory for a Dopplerbroadened signal in presence of an infrared pump

Sharmistha Ghoshal and Pradip N. Ghosh

Citation: The Journal of Chemical Physics **83**, 4015 (1985); doi: 10.1063/1.449116
View online: http://dx.doi.org/10.1063/1.449116
View Table of Contents: http://scitation.aip.org/content/aip/journal/jcp/83/8?ver=pdfcov
Published by the AIP Publishing

Line shape theory for a Doppler-broadened signal in presence of an infrared pump

Sharmistha Ghoshal and Pradip N. Ghosh[a)]
Department of Physics, University of Calcutta, 92, A. P. C. Road, Calcutta-700009, India

(Received 6 March 1985; accepted 29 April 1985)

A theory of line shape for a Doppler broadened probe in the presence of a strong infrared pump is presented. The optical analog of Bloch equations has been developed; the T_1, T_2 relaxations are introduced phenomenologically in these equations. Doppler broadening of both the pump and signal transitions are taken into account to obtain the absorption coefficient for the signal. This leads to a Doppler broadened Gaussian function weighted by a pump induced Lorentzian function whose position and linewidth are controlled by the detuning and power respectively of the pump radiation. The absorption coefficient is further modulated by a Lorentzian function containing the fourth power of the radiation. The off-resonance pumping leads to two symmetrically located "Lamb dips" or "peaks" around the Gaussian pedestal for co- and counter propagating laser radiations. A calculation of the line shape of the central sub-Doppler feature for the on-resonance pumping is in good agreement with the observed variation of linewidth with pressure. Numerical results are presented graphically to demonstrate the pump and signal power dependence of the central hole or peak for the bent and cascade-type double resonances. The results obtained confirm the expected behavior based on level populations.

I. INTRODUCTION

The double resonance methods have been profitably used by microwave spectroscopists for more than a decade. The underlying theory of the method is known from Javan's[1] paper for a three level maser which was formulated well before the experimental realization of the double resonance methods in molecular spectroscopy. In the case of rotational transitions in the microwave region the Doppler broadening is much smaller compared to the line broadening due to collisions. Hence the use of low pressure allows one to obtain extremely narrow lines in the microwave spectra. The difficulty associated with the large crowding of rotational lines in the microwave spectra can be circumvented by using double resonance techniques when one can pick out only those transitions which have one energy level common with the transition that is in resonance with the pump. The presence of a strong pumping radiation can cause a large enhancement of the signal intensity. The line shape of the microwave–microwave double resonance signal has been calculated[2,3] on the basis of Javan's theory for the different values of pump power, as well as for the different values of the off-resonance pumping. In the case of infrared or optical region the large Doppler broadening leads to a broad Gaussian line shape. The appearance of narrow structures on the Doppler broadened spectrum has been investigated by several authors.[4–9] Schlossberg and Javan[4] treated the absorption of two weak monochromatic radiations at closely spaced frequencies lying within the Doppler broadening of the resonance. By means of the third order polarization theory they obtained an appreciable nonlinear coupling between the two fields. This coupling leads to a sharp resonance when the frequency difference between the applied radiations becomes equal to that of two of the components which form either level structure. Tang and Statz[5] also discussed the resonance absorption of two linearly polarized radiations in special situations. Feld and Javan[7] investigated a three level atomic system with a strong pump field and a weak probe field with arbitrary frequencies. They included radiative decay and hard collisions in their theoretical treatment. They also assumed that the pump field fully saturates one transition. The emitted power of the weak probe signal is calculated in terms of the transition rates. Using this so-called transition rate approach they demonstrated the laser-induced line narrowing effect on the Doppler broadened transitions. Hansch and Toschek[10] worked out the theory of a three-level gas laser amplifier on the basis of the density matrix equations by taking account of the level degeneracy, light polarization, and inelastic and dephasing collision. More recently, Takami[11,12] investigated the line shape for the infrared–microwave double resonance for either microwave or infrared used as a weak signal with the other as the pump. They used the density matrix approach and included the two-photon effect. The results predicted holes and peaks on the Doppler broadened Gaussian background for the different level schemes. McGurk *et al.*[13] developed the optical analog of Bloch equations for a two-level system in the presence of a resonating field. A steady state solution leads to the absorption line shape. They also indicated the extension of the theory to a three level system and demonstrated the line shape of the narrow hole sitting on the Gaussian background. They assumed small power for the pump and signal so that the two-photon effects were omitted.

In this paper we consider a general case of two Doppler broadened transitions under the effect of a strong pump and a weak signal. The two laser radiations are incident on a three level system (Fig. 1), both of the radiations being in near resonance with any two of the energy level differences of the system. In such a case we request the following conditions to hold: (1) Both the frequencies are within the Doppler

a)To whom correspondence should be addressed. Physics Department, University College of Science, 92, A.P.C. Road, Calcutta-700 009, India.

 0021-9606/85/204015-09$02.10

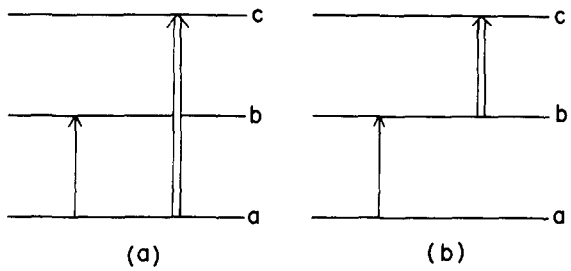

FIG. 1. Energy level configuration for a three level system. The broad and the narrow lines represent the pump and the signal frequencies respectively, (a) bent configuration, (b) cascade configuration.

width of the transitions, so that the frequency detuning is small. (2) The homogeneous linewidths produced by collisions are small, i.e., a low pressure system is used. (3) The Rabi frequency arising from the interaction of the applied electric field with the electric dipole is small so that the magnitude of the coherency splitting is small compared to the transition frequency. (4) The longitudinal and transverse relaxation times are taken into account. The velocity changing collisions are disregarded. (5) The magnitudes of the applied pump and signal fields are considerable but not large enough to produce a dominant two-photon effect. The relaxation effects are introduced in a phenomenological way. A nonlinear term involving the product of the two transition dipole moments is introduced. The calculated line shapes will be used to compare with recent IRIR double resonance features observed in NH_3.[14] The effect of increasing pump and signal powers on the line shape of the sub-Doppler features for the bent and cascade type double resonances will be discussed.

In Sec. II we derive the line shape for the signal transition from the optical Bloch equations of a three level system. The Doppler broadening is included. We also discuss the effect of spatial degeneracy and the collisional transfer of resonance. In Sec. III we present the calculations for a few model three level systems to show the effect of varying pump and signal powers. We also attempt to simulate the line shapes of infrared–infrared double resonance of NH_3 which has been reported in recent experiments.[14] Section IV presents a discussion of line broadening mechanisms.

II. THEORY

A. Optical Bloch equations in three level systems

We consider the molecular gas as an ensemble of nondegenerate three level quantum systems. Two plane-polarized coherent electromagnetic waves are incident on the system. The incident waves are at near resonance with the energy level differences shown in Fig. 1(a), so that

$$\Delta\omega_p = \omega_{0p} - \omega_p \quad \text{and} \quad \Delta\omega_s = \omega_{0s} - \omega_s \tag{1}$$

are small where

$$\omega_{0p} = (E_c - E_a)/\hbar \quad \text{and} \quad \omega_{0s} = (E_b - E_a)/\hbar. \tag{2}$$

The perturbed Hamiltonian of the three level system under the influence of the two electromagnetic fields, with the intensities ϵ_p and ϵ_s and the frequencies ω_p and ω_s, respectively, is

$$H = H_0 - 2\mu\epsilon_p \cos\omega_p t - 2\mu\epsilon_s \cos\omega_s t, \tag{3}$$

where μ is the dipole moment operator. The density matrix σ for the Hamiltonian in Eq. (3) satisfies the following rate equation:

$$i\hbar\frac{\partial\sigma}{\partial t} = [H,\sigma], \tag{4}$$

where relaxation effects are not included. If ρ is the density matrix in the interaction representation, then we get the following rate equations for the components of ρ under the rotating wave approximation:

$$i\hbar\frac{\partial}{\partial t}\rho_{aa} = \epsilon_s(\rho_{ab}\mu_{ba} - \mu_{ab}\rho_{ba}) + \epsilon_p(\rho_{ac}\mu_{ca} - \mu_{ac}\rho_{ca}), \tag{5a}$$

$$i\hbar\frac{\partial}{\partial t}\rho_{bb} = \epsilon_s(\rho_{ba}\mu_{ab} - \mu_{ba}\rho_{ab}), \tag{5b}$$

$$i\hbar\frac{\partial}{\partial t}\rho_{cc} = \epsilon_p(\rho_{ca}\mu_{ac} - \mu_{ca}\rho_{ac}), \tag{5c}$$

$$i\hbar\frac{\partial}{\partial t}\rho_{ab} = \epsilon_s\mu_{ab}(\rho_{aa} - \rho_{bb}) - \epsilon_p\mu_{ac}\rho_{cb} - \rho_{ab}\hbar\Delta\omega_s, \tag{5d}$$

$$i\hbar\frac{\partial}{\partial t}\rho_{bc} = \rho_{bc}\hbar(\Delta\omega_s - \Delta\omega_p) - \epsilon_s\mu_{ba}\rho_{ac} + \epsilon_p\rho_{ba}\mu_{ac}, \tag{5e}$$

$$i\hbar\frac{\partial}{\partial t}\rho_{ac} = \epsilon_p\mu_{ac}(\rho_{aa} - \rho_{cc}) - \epsilon_s\mu_{ab}\rho_{bc} - \rho_{ac}\hbar\Delta\omega_p. \tag{5f}$$

We have assumed in the above that the transitions $a \rightarrow b$ and $a \rightarrow c$ are dipole allowed. Under the effect of the applied electromagnetic field the molecular dipoles will be oriented towards the field direction and a macroscopic polarization will develop

$$P = N\,\mathrm{Tr}(\mu\sigma), \tag{6}$$

where N is the number of molecules per unit volume. Using the interaction representation for the density matrix we get

$$P = N\{\mu_{ca}\rho_{ac}\exp(i\omega_p t) + \mu_{ba}\rho_{ab}\exp(i\omega_s t) + \text{c.c.}\}. \tag{7}$$

The above expression allows us to introduce the real and imaginary parts of the polarization associated with the pump and signal as follows:

$$P_{pr} + iP_{pi} = \mu_{ca}\rho_{ac}, \tag{8a}$$

$$P_{sr} + iP_{si} = \mu_{ba}\rho_{ab}. \tag{8b}$$

Further we introduce a nonlinear term involving the nondiagonal element ρ_{bc} and corresponding to the product of the two transition dipoles[11]

$$P_{nr} + iP_{ni} = \mu_{ca}\mu_{ab}\rho_{bc}. \tag{8c}$$

We also define

$$\Delta N_p = N(\rho_{aa} - \rho_{cc}),$$

$$\Delta N_s = N(\rho_{aa} - \rho_{bb}).$$

With these definitions and using the rate equations for the density matrix we obtain the optical analog of the Bloch equations:

$$\frac{d}{dt}P_{pr} + \Delta\omega_p P_{pi} + \frac{\epsilon_s}{\hbar}P_{ni} + \frac{P_{pr}}{T_{2p}} = 0, \tag{9a}$$

$$\frac{d}{dt}P_{pi}+\epsilon_p K_1^2\left(\frac{\hbar}{4}\Delta N_p\right)$$

$$-\frac{\epsilon_s}{\hbar}P_{nr}-\Delta\omega_p P_{pr}+\frac{P_{pi}}{T_{2p}}=0, \tag{9b}$$

$$\frac{d}{dt}\left(\frac{\hbar}{4}\Delta N_p\right)-\epsilon_p P_{pi}-\tfrac{1}{2}\epsilon_s P_{si}$$

$$+\frac{\hbar}{4}\frac{\Delta N_p-\Delta N_{op}}{T_{1p}}=0, \tag{9c}$$

$$\frac{d}{dt}P_{sr}+\Delta\omega_s P_{si}-\frac{\epsilon_p}{\hbar}P_{ni}+\frac{P_{sr}}{T_{2s}}=0, \tag{9d}$$

$$\frac{d}{dt}P_{si}-\Delta\omega_s P_{sr}+\epsilon_s K_2^2\left(\frac{\hbar}{4}\Delta N_s\right)$$

$$-\frac{\epsilon_p}{\hbar}P_{nr}+\frac{P_{si}}{T_{2s}}=0, \tag{9e}$$

$$\frac{d}{dt}\left(\frac{\hbar}{4}\Delta N_s\right)-\epsilon_s P_{si}-\tfrac{1}{2}\epsilon_p P_{pi}+\frac{\hbar}{4}\frac{\Delta N_s-\Delta N_{0s}}{T_{1s}}=0, \tag{9f}$$

$$\frac{d}{dt}P_{nr}-(\Delta\omega_s-\Delta\omega_p)P_{ni}+\frac{\epsilon_p}{\hbar}|\mu_{ac}|^2P_{si}$$

$$+\frac{\epsilon_s}{\hbar}|\mu_{ab}|^2P_{pi}+\frac{P_{nr}}{T_{2n}}=0, \tag{9g}$$

$$\frac{d}{dt}P_{ni}+(\Delta\omega_s-\Delta\omega_p)P_{ni}-\frac{\epsilon_s}{\hbar}|\mu_{ab}|^2P_{pr}$$

$$+\frac{\epsilon_p}{\hbar}|\mu_{ac}|^2P_{sr}+\frac{P_{ni}}{T_{2n}}=0, \tag{9h}$$

where

$$K_1=\frac{2\mu_{ac}}{\hbar}\quad\text{and}\quad K_2=\frac{2\mu_{ab}}{\hbar}.$$

Above we have introduced collisional relaxation times T_2 and T_1 for the polarization and the population differences, respectively, in a phenomenological way. We also introduce a relaxation time T_{2n} for the nonlinear terms P_{nr} and P_{ni}. When the perturbing radiations are withdrawn all the polarization terms decay to their equilibrium values of zero and the population differences ΔN_p and ΔN_s decay to the equilibrium values of ΔN_{0p} and ΔN_{0s}, respectively.

B. Doppler broadening

Considering the molecules to be in motion either along or opposite to the direction of propagation of electromagnetic radiations with velocity v we replace $\Delta\omega_p$ and $\Delta\omega_s$ by

$$\Delta\omega_p'=\Delta\omega_p+\chi r\omega', \tag{10a}$$

$$\Delta\omega_s'=\Delta\omega_s+\omega', \tag{10b}$$

where $\omega'=\omega_s v/c$, $r=\omega_p/\omega_s$ and $\chi=+1$ or -1, when the two radiations are traveling in the same or opposite directions. Hence the polarization terms are functions of molecular velocity. The coefficient of absorption for signal transition is defined as

$$\gamma(v,\omega_s)=\frac{-4\pi\omega_s}{c}\frac{P_{si}(v,\omega_s)}{\epsilon_s}. \tag{11}$$

Assuming a Maxwell velocity distribution, the total absorption coefficient is

$$\gamma(\omega_s)=\frac{q}{\pi^{1/2}}\int_{-\infty}^{+\infty}e^{-q^2\omega'^2}\gamma(v,\omega_s)d\omega', \tag{12}$$

where

$$q=\sqrt{\ln 2}/\Delta\omega_D \tag{13}$$

and

$$\Delta\omega_D=\frac{\omega_s}{c}\sqrt{\frac{2kT\ln 2}{M}} \tag{14}$$

is defined as the Doppler half-width at temperature T and M is the molecular weight.

C. Steady state solution

We are interested in double resonance experiments with two continuous wave lasers. Hence we consider the steady state solutions of Eq. (9). Substituting the solution for P_{si} in Eqs. (11) and (12) we obtain

$$\gamma(\omega_s)=\frac{\hbar\pi^{1/2}\omega_s qK_2^2}{c}\int d\omega'\,e^{-q^2\omega'^2}$$

$$\times\left[\Delta N_{0s}\left\{\frac{1}{T_{2p}}+x_p^2T_{1p}+\Delta\omega_p'^2T_{2p}\right\}\right.$$

$$\left.-\tfrac{1}{2}x_p^2\Delta N_{0p}\{T_{1s}+\tfrac{1}{2}T_{2n}\}\right]/M_1, \tag{15}$$

where the denominator M_1 is

$$M_1=\left[\left\{\left(\frac{1}{T_{2p}}+x_p^2T_{1p}+\Delta\omega_p'^2T_{2p}\right)\right.\right.$$

$$\left.\times\left(\frac{1}{T_{2s}}+x_s^2T_{1s}+\frac{1}{4}x_p^2T_{2n}+\Delta\omega_s'^2T_{2s}\right)\right\} \tag{16}$$

$$\left.-\tfrac{1}{4}x_p^2x_s^2T_{1p}(T_{1s}+\tfrac{1}{2}T_{2n})\right]$$

and

$$x_p=\epsilon_pK_1\ \text{ and }\ x_s=\epsilon_sK_2. \tag{17}$$

We have also assumed that the relaxation of the nonlinear term is much faster than that of the linear terms so that T_{2n} is much smaller compared to T_{2s} and T_{2p}. Further we assume a small signal power so that $x_sT_{2s}<1$. We also assume that the Doppler width $\Delta\omega_D$ is large compared to the collisional broadening. In the limit of the large T_{2s} we can approximate

$$\frac{1/T_{2s}}{1/T_{2s}^2+(\Delta\omega_s')^2+x_s^2T_{1s}/T_{2s}+\tfrac{1}{4}x_p^2T_{2n}/T_{2s}}$$

$$=\pi\delta(\omega_{0s}-\omega_s+\omega'). \tag{18}$$

From Eqs. (15) and (18) we get the total absorption coefficient as

$$\gamma(\omega_s) = \frac{\pi^{3/2}\hbar K_2^2 \omega_s q}{c} \exp[-q^2(\omega_s - \omega_{0s})^2]$$
$$\times \left\{ \Delta N_{0s} - \frac{\Delta N_{0p} x_p^2 (T_{1s} + \frac{1}{2}T_{2n})/2}{[(1/T_{2p}) + \{w_{0p} - \omega_p + \chi r(\omega_s - \omega_{0s})\}^2 T_{2p} + x_p^2 T_{1p}]} \right\} \tag{19}$$
$$\times \left\{ 1 + \frac{x_p^2 x_s^2 T_{1p}(T_{1s} + \frac{1}{2}T_{2n})/4}{\{(1/T_{2s} + x_s^2 T_{1s} + \frac{1}{4}x_p^2 T_{2n}\}\{(1/T_{2p}) + x_p^2 T_{1p} + (\omega_{0p} - \omega_p + \chi r(\omega_s - \omega_{0s}))^2 T_{2p}\}} \right\}.$$

When the pump and signal powers are small, the nonlinear terms in the polarization will be insignificant. In such a case the term containing $x_p^2 x_s^2$ in Eq. (19) may be neglected. In this case the expression for $\gamma(\omega_s)$ reduces to the absorption coefficient calculated by McGurk *et al.*[13] for steady state double resonance where the two-photon effects are completely omitted. Thus the signal line shape for low incident powers is given by a Gaussian curve modulated by a Lorentzian hole whose width is determined by the factor $[(1/T_{2p}^2) + x_p^2(T_{1p}/T_{2p})]^{1/2}$ and whose amplitude is governed by $x_p^2(T_{1p}/T_{2p})$. In the case of infrared spectroscopy the linewidth of the hole is much small compared to the Doppler width expressed by q. When the power levels are increased so that the two-photon effects cannot be neglected, we have to consider the full expression given by the Eq. (19). The additional factor in Eq. (19) will lead to further modification of the saturation dip. In the present three-level scheme the effect of the additional nonlinear term is to lower the amplitude of the Lorentzian hole. The line shape of the hole is given by a Lorentzian when the Doppler broadening is large. The inclusion of the terms containing $x_p^2 x_s^2$ in the numerator will lead to a change in the line shape since the resultant line shape is given by a convolution of the two Lorentzian functions. However, this effect is very small since the net contribution from this term is of the order of x_s^2.

Instead of the level scheme given in Fig. 1(a) which is known as type I or bent type double resonance we may have a level scheme shown in Fig. 1(b), which corresponds to type II or cascade type double resonance. In the case of type II, we can derive the formula of $\gamma(\omega_s)$ in the same way and the result is an expression for $\gamma(\omega_s)$ given by Eq. (19) with $(\Delta N_{0p}/\Delta N_{0s})$ replaced by $-(\Delta N_{0p}/\Delta N_{0s})$. This means that instead of getting a Lorentzian hole burned on the Doppler broadened absorption profile we get a Lorentzian peak sitting on the Gaussian pedestal.

D. Spatial degeneracy

The three-level scheme presented above considers nondegenerate energy levels. The formulation is applicable to molecular vibration-rotation energy levels (v, J,k). However, these levels have $(2J + 1)$-fold spatial degeneracy as well as spin degeneracy. If we exclude from the treatment the effect of the nuclear quadrupole effects and the symmetry of internal roters, if any, which produces near degeneracies we can consider the effect of this spatial degeneracy on the line shape.

In the absence of Stark field the calculation of the transition dipole moment has to take account of the double resonance processes as given in Fig. 2 when the pump and signal radiations are polarized perpendicular to each other. Figures 2(a) and 2(b) represent the two possible combinations of selection rules: (a) $\Delta M_p = 0$ and $\Delta M_s = \pm 1$ and (b) $\Delta M_p = \pm 1$ and $\Delta M_s = 0$. Thus the line shape of the observed double resonance signal is obtained by summing the absorption coefficients of the transitions shown in the Fig. 2. All of these transitions have the same frequencies for both the pump and the signal transitions. Their absorption coefficients differ by the values of μ_{ac} and μ_{ab} which may easily be calculated for a particular $JkM \rightarrow J'k'M' =$ transition.[15,16]

In the case of Stark-tuned double resonance the energy levels with different M values are split up. For the second order Stark splitting the different types of DR signals that may arise may be represented as follows:

$$\Delta M_p = 0, \quad \Delta M_s = \pm 1.$$

If the common level has $|M| = J$ the transitions are $\pm J \rightarrow \pm J, \pm J \rightarrow \pm (J-1)$, these two signals have the same frequencies and we get a single double resonance signal for the pumping as depicted in Fig. 3(a). When $M = 0$ we get $\Delta M_p = 0$, $\Delta M_s = \pm 1$ thus giving only one DR signal for $M = 0 \rightarrow 0$ pumping as shown in Fig. 3(b). When $0 < |M| < J$, for each pumping frequency one observes two double resonance signals each of which consists of two different double resonance processes shown in Figs. 3(c) and 3(d).

$$\Delta M_p = \pm 1, \quad \Delta M_s = 0.$$

For $\Delta|M_p| = 1$ we get two double resonance processes $\pm(J-n-1) \rightarrow \pm(J-n)$, $\pm(J-n-1) \rightarrow \pm(J-n-1)$ having the same frequencies as depicted in Fig. 4(a). Similarly for $\Delta|M_p| = -1$ we get a signal from the processes shown in Fig. 4(b).

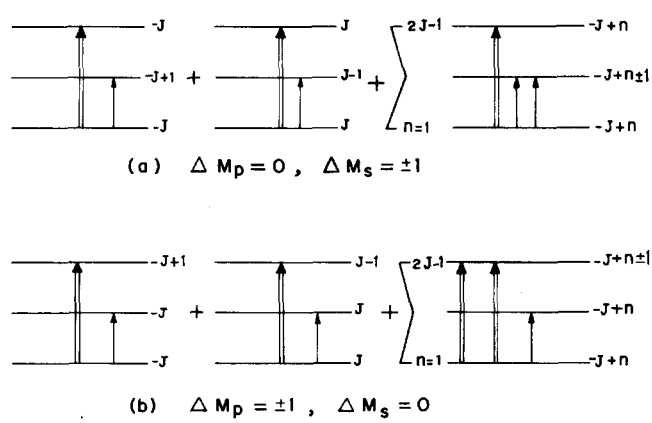

FIG. 2. Energy level scheme to show the DR transitions including the spatial degeneracy in absence of the Stark field for (a) $\Delta M_p = 0$ and $\Delta M_s = \pm 1$ and (b) $\Delta M_p = \pm 1$ and $\Delta M_s = 0$.

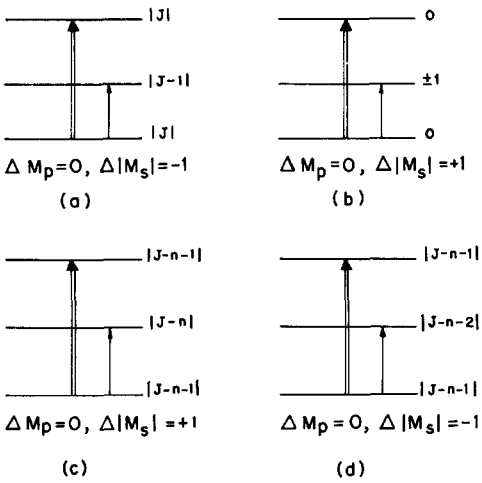

FIG. 3. Energy level scheme to show the DR transitions including the spatial degeneracy in the presence of the Stark field for (a) $\Delta M_p = 0$, $\Delta|M_s| = -1$, (b) $\Delta M_p = 0$, $\Delta|M_s| = +1$, (c) $\Delta M_p = 0$, $\Delta|M_s| = +1$, and (d) $\Delta M_p = 0$, $\Delta|M_s| = -1$ and $n = 0,1,\ldots, J-2$ in (c) and (d) and $J>2$.

We have so far considered the on-resonance pumping effects on the signal. However, in the presence of the Stark field along with the on-resonance pumping, there would be a few cases of off-resonance pumping since the M levels are very closely spaced. The line shapes for these cases are also obtained from Eq. (19). For the on-resonance pumping ($\Delta\omega_p = 0$), the maximum of the Lorentzian dip is at $\omega_s = \omega_{0s}$ giving a central dip where the dips corresponding to the copropagating and the counterpropagating waves coincide. For the off-resonance pumping the dips are obtained from

$$\omega_s - \omega_{0s} = \frac{(\omega_p - \omega_{0p})}{\chi r}. \tag{20}$$

Thus there are two dips symetrically located on the two sides of the resonance frequency ω_{0s}. The spacing between them is determined by the magnitude of the off-resonance pumping $\Delta\omega_p$ and the frequency ratio ω_p/ω_s. In such cases, at signal resonance $\omega_s = \omega_{0s}$, the pumping effect on the signal frequency is small because of the larger denominator. This would give rise to the normal peak height of the Doppler absorption curve. The fractional height of the Lorentzian dip is the same as in the case of the on-resonance pumping, but the actual height of the dip becomes much smaller because the signal is off resonance.

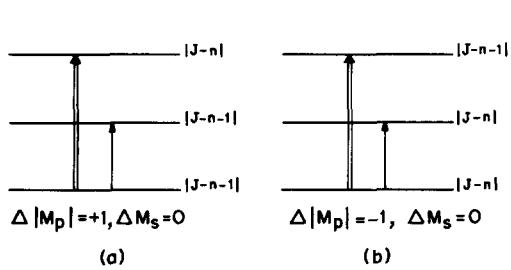

FIG. 4. Energy level configuration for the DR transitions including spatial degeneracy in the presence of the Stark field for (a) $\Delta|M_p| = +1$, $\Delta M_s = 0$, (b) $\Delta|M_p| = -1$, $\Delta M_s = 0$, $n = 0,1,\ldots, J-1$ and $J>1$.

E. Transfer of resonances

The above formulation of the signal line shape in the presence of the off-resonance pumping does not include the fact that the off-resonance pumping frequency may itself be on resonance with another energy level difference. This is often true in the case of the Stark-tuned double resonance experiments as discussed earlier. In such a case one has to consider the collisional transfer of resonances between the pairs of energy levels. These transfers are associated with change of the states but the velocity is preserved.[17–19] In the case of type I double resonance (Fig. 5) the collisions transfer the resonances between $(a \rightarrow c)$ and $(d \rightarrow f)$. We consider the transfer induced by the on-resonance $(a \rightarrow c)$ pumping to the level populations of d and f. We can write

$$\rho_{dd} = \rho^0_{dd} + f(\rho_{aa} - \rho^0_{aa}), \tag{21a}$$

$$\rho_{ff} = \rho^0_{ff} + f(P_{cc} - \rho^0_{cc}), \tag{21b}$$

where ρ^0_{aa} and ρ^0_{cc} describe the populations in the levels a and c in the absence of pumping, ρ^0_{dd} and ρ^0_{ff} describe the populations in the absence of collisional transfer, f is the transfer coefficient. The change in population difference produced by the pumping is controlled by the pump power ϵ_p and the transition probability μ_{ac}. If the population difference $(N_a - N_c)$ is reduced to a fraction F of its equilibrium value $(N^0_a - N^0_c)$ by pumping we get

$$\Delta N^1_{0p} = \Delta N_{0p} - f(1-F)N^0_a\left[1 - \exp\left(-\frac{h_p}{kT}\right)\right] \tag{22}$$

for the population difference of the levels d and f in the presence of collisional transfer induced by the pumping. Similarly, the signal population difference ΔN^1_{0s} in the presence of the transfer is given by

$$\Delta N^1_{0s} = \Delta N_{0s} - \tfrac{1}{2}f(1-F)N^0_a\left[1 - \exp\left(-\frac{h_p}{kT}\right)\right]. \tag{23}$$

There is no transfer to the level e. These changes in the population differences may be introduced in Eq. (19) to find the effect of resonance transfer of pumping on the sub-Doppler features. The change in $\Delta N_{0p}/\Delta N_{0s}$ will cause an appreciable change in the peak height of the Lamb dip.

III. CALCULATIONS

We have calculated the signal absorption coefficients [Eq. (19)] for the two types of double resonances shown in Fig. 1 to demonstrate the effect of the varying pump and signal powers on the line shape, particularly the sub-Doppler features. We also present simulation of the double resonance line shapes in NH_3 as has been studied recently by infrared–infrared double resonance experiments.[14]

Figure 6 shows the absorption line shape for a fixed value of signal power and varying pump powers. We have used

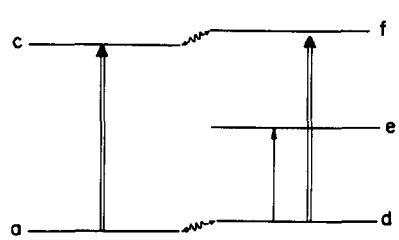

FIG. 5. Energy level diagram showing the collisional transfer of pumping.

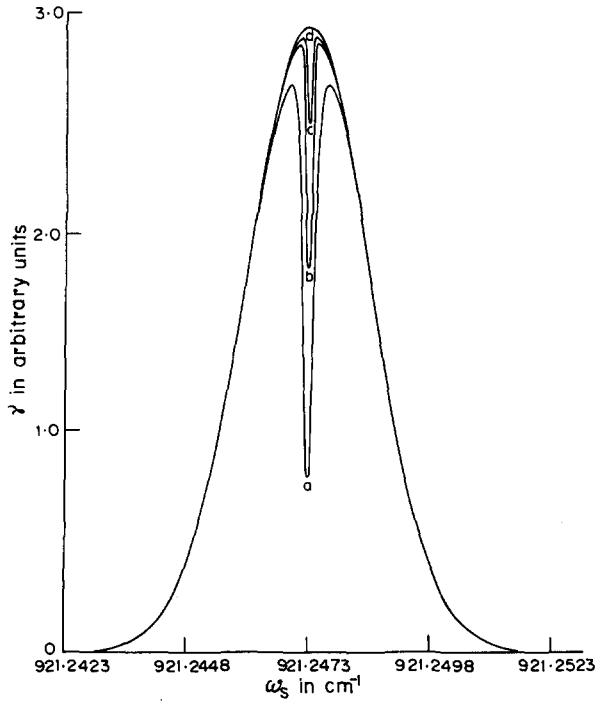

FIG. 6. Line shape of infrared–infrared double resonance for the bent configuration [Fig. 1(a)] for a fixed value of $x_s\tau = 0.1$ and the values of $x_p\tau$ of (a) 4.0, (b) 1.0, (c) 0.5, and (d) 0.0.

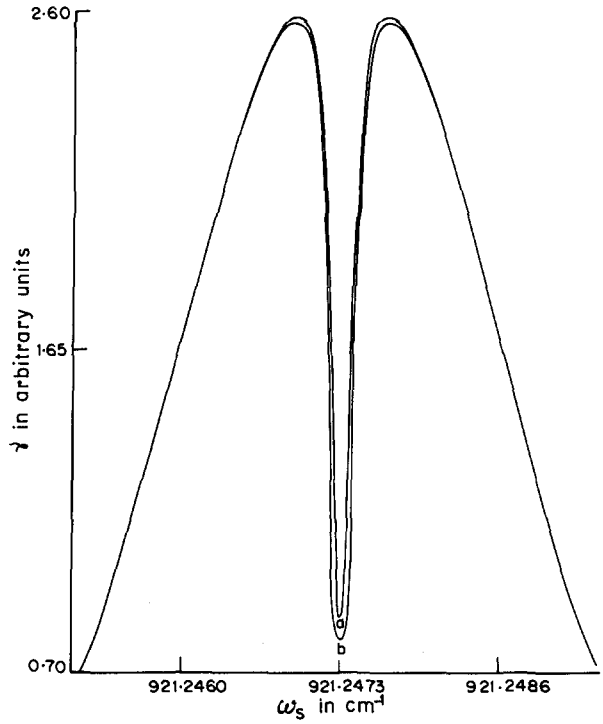

FIG. 7. Line shape of infrared–infrared double resonance for the bent configuration [Fig. 1(a)] for a fixed value of $x_p\tau = 4.0$ and the values of $x_s\tau$ of (a) 0.7 and (b) 0.1.

the signal frequency $\omega_{0s} = 921.2550\,\text{cm}^{-1}$ corresponding to the $\nu_2[aQ\ (9,9)]$ transition and $\omega_{0p} = 1775.2674\,\text{cm}^{-1}$ corresponding to the $\nu_4[a^R R\ (9,9)]$ transition of NH_3.[14] We assume $T_{1s} = T_{2s} = T_{1p} = T_{2p} = \tau$ and T_{2n} is much smaller compared to τ. The value of τ is taken approximately as 0.7 μs.[20] We also have $q = 558$ per cm^{-1} at the temperature $T = 300$ K which corresponds to a Doppler half-width of 80 MHz approximately and $\Delta N_{0p}/\Delta N_{0s} = 1.53$ from the Boltzmann distribution. The transition dipole moment for the signal is taken as 0.23 D.[21] The pump is assumed to be on resonance so that we get the central sub-Doppler features. It is found that the height and the half-width of the central dip increases with increasing pump power. When $x_p\tau$ is very large the half-width becomes large and the peak height reaches saturation. In Fig. 7 we present similar calculations for a fixed value of the pump power and varying signal powers. It is noticeable that the height and the half-width of the dip decreases with increasing $x_s\tau$. This may be associated with the relatively lower pumping rate for the stronger signal radiation. However, the overall feature of these curves is that the signal power has a relatively small effect on the double resonance line shape and it arises from the additional term in Eq. (19) which corresponds to the two-photon effect. It may be noted that our formulation of Eq. (19) sets an upper limit to the value of x_s. Hence the effect of the larger signal power could not be ascertained. Nevertheless, the double resonance process itself precludes the use of high signal power. The model calculations presented above are aimed at demonstrating the effect of the radiation powers on the DR line shape. Hence we have assumed the energy levels to be single and no effect of spatial degeneracy is considered.

Figures 8 and 9 represent similar calculations carried out for the double resonance of the cascade type shown in Fig. 1(b). We have used $\omega_{0s} = 1035.4426\,\text{cm}^{-1}$ corresponding to the $\nu_2[asQ\ (5,3)]$ transition and $\omega_{0p} = 1053.8802\,\text{cm}^{-1}$ corresponding to the $\nu_2[ssR\ (5,3)]$ transition of NH_3.[22] The other parameters are kept the same except for the fact that

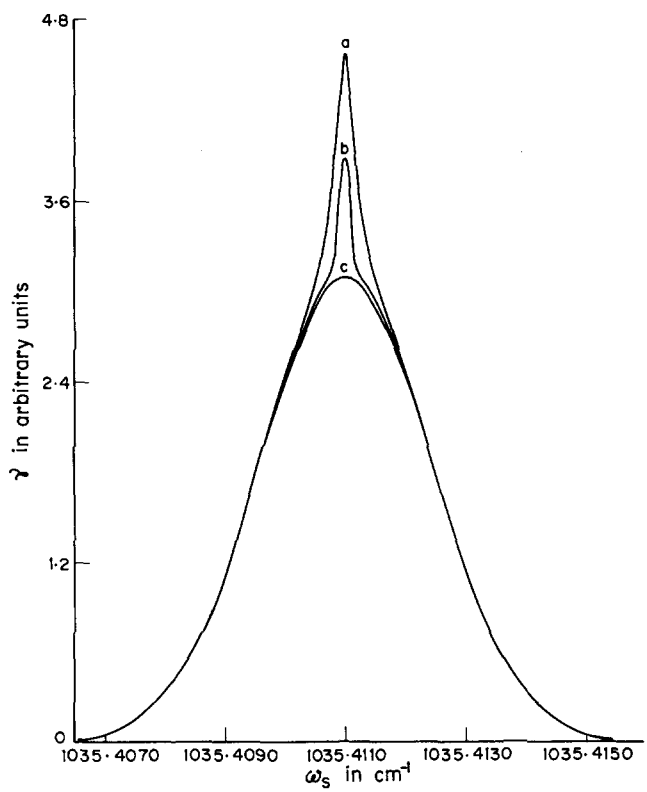

FIG. 8. Line shape of infrared–infrared double resonance for the cascade configuration [Fig. 1(b)] for a fixed value of $x_s\tau = 0.1$ and the values for $x_p\tau$ of (a) 4.0, (b) 1.0, and (c) 0.0.

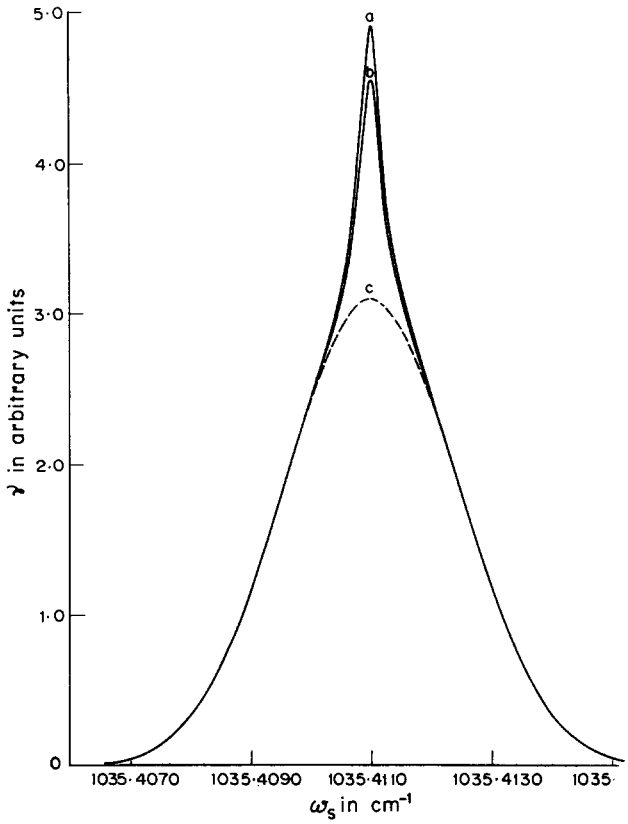

FIG. 9. Line shape of infrared–infrared double resonance for the cascade configuration [Fig. 1(b)] for a fixed value of $x_p\tau = 4.0$ and the values for $x_s\tau$ of (a) 0.7 and (b) 0.1. The curve (c) represents the Gaussian background when $x_p\tau = 0$.

$\Delta N_{0p}/\Delta N_{0s} = 1.013$ in this case. In Fig. 8 we have plotted the signal line shapes for a fixed value of the signal power and varying pump powers. In this case we obtain an inverted Lamb dip or peak sitting on the top of the Gaussian pedestal. This sub-Doppler feature also increases in height and half-width with the increasing pump power. Figure 9 shows the line shapes for the fixed value of $x_p\tau$ and varying signal powers $x_s\tau$. The figure also includes a case for $x_p\tau = 0$ to show the location of the Gaussian pedestal. In this case the peak height of the central sub-Doppler feature increases with increasing signal power, contrary to what was observed in the other case (Fig. 7). This may be due to the larger population of the upper signal or lower pump level caused by the large signal power. In the work of McGurk *et al.*[13] the signal power was assumed to be negligible hence the signal power dependence of the line shape could not be ascertained from their work.

We have also attempted to simulate the line shape for the Stark-tuned DR signals $\nu_2[aQ\ (9,9)]$ and $\nu_2[aQ\ (7,7)]$ of NH_3 observed by pumping the transitions $\nu_4[a^RR\ (9,9)]$ and $\nu_4[a^RR\ (7,7)]$, respectively.[14] In the former case the pump radiation is locked to the $M = 9 \rightarrow 10$ component of the $\nu_4[a^RR\ (9,9)]$ transition at $\omega_{0p} = 1775.2674\ \text{cm}^{-1}$ and the signal line shapes are calculated for the $M = 7$, 8, and 9 Stark components ($\Delta M = 0$) of the $\nu_2[aQ\ (9,9)]$ transition. Thus the $M = 9$ component of the signal is pumped on-resonance and the others are pumped off-resonance. The on-resonance pumping case corresponds to Fig. 4(a) where the effects of the two signals arising from the double degeneracy are included. The values of x_p and x_s may be calculated from the known laser powers and the transition moments. The laser powers used in the experiment were 10 W/cm^2 for pump[14] and approximately 1 mW/cm^2 for the signal.[23] However, the value of μ_{ac} for the relevant Stark component becomes difficult to determine. The pump laser-induced line shape for the transmission change $\Delta T/T$ of the $M = 9$ central Lamb dip has a full width at half maximum (FWHM) of 3.2 ± 0.15 MHz at a pressure of 10 mTorr and a pump power of 8 W/cm^2. Our expression for the absorption coefficient shows that the half-width at half maximum (HWHM) of the sub-Doppler feature is roughly given by $(x_p^2 + 1/\tau^2)^{1/2}$. From the pressure broadening coefficient of 25 MHz/Torr of NH_3,[24] we obtain $1/\tau = 0.25$ MHz at 10 mTorr. The observed linewidth includes contributions also from the beam divergence, the field inhomogeneity and the laser linewidth in addition to the pressure and power broadening. Our formulation does not include these effects. Weber and Terhune[14] discussed these broadening mechanisms and their estimates give the transit time broadening as 0.16 MHz and the broadening due to the field inhomogeneity as 1% of the Doppler broadening, i.e., 0.8 MHz. The linewidth of the diode laser is estimated to be 1 MHz or less. Considering all these facts we obtain the power broadening due to pumping as $x_p = 0.57$ MHz. At a pressure of 30 mTorr, we obtain $1/\tau = 0.75$ MHz. With the value of $x_p = 0.57$ MHz we obtain a FWHM of 3.5 MHz which is in good agreement with the observed FWHM of 3.8 MHz at 30 mTorr. In the case of the $M = 7$ and 8 components the calculated line shapes show two sub-Doppler features symmetrically located around the central Gaussian. The magnitude of the off-resonance pumping frequency is determined by the Eq. (20) and the observed value[14] of $(\omega_s - \omega_{0s})$. The line shapes have Doppler widths of nearly 80 MHz for each of the components. We have convoluted these lineshapes and this is reproduced in Fig. 10. The values of x_p and $1/\tau$ used in this calculation correspond to the pump power of 10 W/cm^2 and pressure of 30 mTorr. The relative heights of the Stark components[15] are taken to be proportional to M^2. There is very good agreement of the sub-Doppler features with the observed curve regarding their relative heights and half-widths.[14] However, the overall line shape of the spectrum cannot be compared with the observed line shape. In the observed curve the maximum of the absorption is at the $M = 9$ component, whereas in the computed line shape this is at a frequency intermediate between the $M = 9$ and $M = 8$ components. One reason for this may be because of the fact that the base line of the observed spectrum is not clearly defined. However, it may also be noted that a convolution of three Gaussian curves each having a width of 80 MHz and frequency spacing of the order of 50 MHz with intensity ratio of 1:0.80:0.60 would not yield a line shape shown in the observed curve. The observed curve is obtained by searching the strong signals with a peak-finding computer programme and finally interpolating between them. This process might have resulted in a loss of the overall line shape. Regarding the line shape of the sub-Doppler features we would also note that we have not taken account of the collisional transfer of resonances as discussed

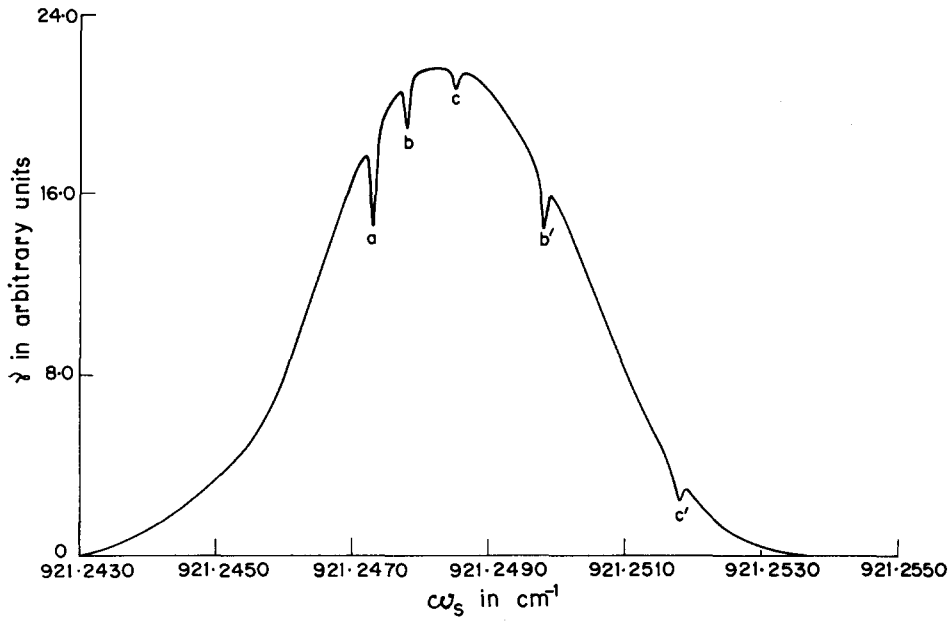

FIG. 10. Computed line shape for the $\nu_2[aQ\ (9,9)]$ signal of NH_3 pumped by the $M = 9 \rightarrow 10$ component of the $\nu_4[a^R R\ (9,9,)]$ transition. The sub-Doppler feature (a) represents the on-resonance $M = 9$ component, while (b,b') and (c,c') represent the off-resonance $M = 8$ and 7 components.

in Sec. II E. The change in the population difference would also modify the shape of the DR features. The evaluation of these effects is not feasible at the moment because of our lack of knowledge of the transfer coefficients. The best way to do that would be to fit the line shape to obtain these data. However, the experimental data are insufficient for doing that.

The same calculations have also been performed for the $\nu_4[a^R R\ (7,7)]$ pump and the $\nu_2[aQ\ (7,7)]$ signal transitions of NH_3.[14] These are reproduced in Fig. 11. The pumping frequency is locked to the $(7 \rightarrow 8)$ component at $\omega_{0p} = 1754.9804\ \text{cm}^{-1}$, the pump power is 6 W/cm^2 and the pressure is 34 mTorr. For evaluation of x_p we have calculated μ_{ac} for the pumping $J\,k\,M = 7,7,7 \rightarrow 8,8,8$ from the value of μ_{ac} obtained earlier for the $(9,9,9 \rightarrow 10,10,10)$ pumping. Because of the large Stark field used in this experiment the separation between the M components is large, hence there is no overlap between the Doppler produced Gaussian backgrounds. The relative heights of these signals agree with the experimental observation. Only the on-resonance pumping case show a central Lamb dip. For the other Stark components the sub-Doppler features would be far from the central frequency ω_{0s} and may be well beyond the Doppler profile. Hence they will not be seen. Again the probability of collisional transfer of resonances in this case would be much small compared to the case presented in Fig. 10 because of the larger separation of the M levels. The inclusion of this transfer would lead to a change in the relative height and width of the DR features of Figs. 10 and 11.

IV. DISCUSSION

The pumping by an infrared laser produces narrow sub-Doppler features on the Gaussian background which is normally obtained from diode laser spectroscopy of gaseous molecules. This provides an opportunity of studying the dif-

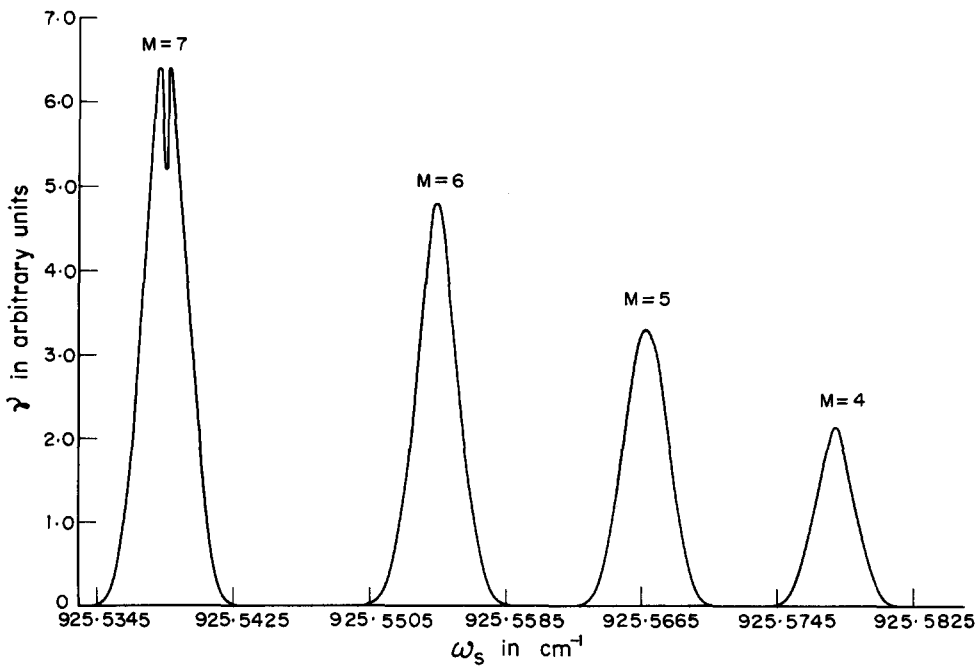

FIG. 11. Computed line shape for the $\nu_2[aQ\ (7,7)]$ signal of NH_3 pumped by the $M = 7 \rightarrow 8$ component of the $\nu_4[a^R R\ (7,7)]$ transition of NH_3.

ferent kinds of line broadening mechanism. The pressure and power broadening can be evaluated from the steady state solution of the optical Bloch equations. The pressure broadening is introduced phenomenologically in terms of the relaxation times. The power broadening is contained in the density matrix equations. A careful study of the power broadening effects have been presented to show how the experimental line shape can degrade with the power when the other broadening mechanisms remain unchanged. The effect of the signal power on the peak height of the sub-Doppler feature is also studied. In addition to the broadening produced by the pump power and the pressure there are other kinds of broadening effects in the observed line shape which are not accommodated in the theoretical derivation. It is intriguing that in spite of the monochromatic character of the laser radiation it has a linewidth which is a sizable fraction of the observed linewidth.

In a highly stable laser the radiation linewidth of the order of 100 kHz arises mainly from the acoustical and mechanical perturbations of the cavity length.[25] The perturbations are usually uncontrollable and consist of a discrete set of frequencies. Qualitatively, we consider the laser frequency to be modulated by a single frequency such that

$$\omega'(t) = \omega + \eta \cos pt, \tag{24}$$

where η is the frequency fluctuation and p is the modulation frequency. When η is small this would add an extra $\eta^2/2$ term to the square of the linewidth $x_p^2 + 1/\tau^2$. When η is of the order of magnitude of x_p this effect becomes more complicated. We have eliminated this effect by assuming it to be additive. The other broadening effects like the beam inhomogeneity and the transit time have been discussed by Weber and Terhune[14] and have to be accounted for in phenomenological ways.

What is more difficult is to evaluate the effect of collisional transfer from nearby energy levels. This is very often encountered in molecular spectroscopy. Evaluation of these effects needs more experimental studies. We have indicated the effect of spatial degeneracy in the case of both zero and nonzero Stark fields. Inclusion of these processes would modify x_p and x_s thereby affecting the line shape.

[1] A. Javan, Phys. Rev. **107**, 1579 (1957).
[2] J. Ekkers, A. Bauder, and Hs. H. Günthard, J. Phys. E **8**, 819 (1970).
[3] J. G. Baker, *Modern Aspects of Microwave Spectroscopy*, edited by G. W. Chantry (Academic, New York, 1979), p. 65.
[4] H. R. Schlossberg and A. Javan, Phys. Rev. **150**, 267 (1960).
[5] C. L. Tang and H. Statz, Phys. Rev. **128**, 1013 (1962).
[6] M. S. Feld and A. Javan, Phys. Rev. Lett. **20**, 578 (1968).
[7] M. S. Feld and A. Javan, Phys. Rev. **177**, 540 (1969).
[8] S. G. Rautian, Sov. Phys. JETP **24**, 788 (1967).
[9] S. G. Rautian and I. I. Sobel'man, IEEE J. Quantum Electron. **QE2**, 446 (1966).
[10] Th. Hansch and P. Toschek, Z. Phys. **236**, 213 (1970).
[11] M. Takami, Jpn. J. Appl. Phys. **15**, 1063 (1976).
[12] M. Takami, Jpn. J. Appl. Phys. **15**, 1889 (1976).
[13] J. C. McGurk, T. G. Schmalz, and W. H. Flygare, Adv. Chem. Phys. **25**, 1 (1974).
[14] W. H. Weber and R. W. Terhune, J. Chem. Phys. **78**, 6437 (1983).
[15] H. W. Kroto, *Molecular Rotation Spectra* (Wiley, London, 1975).
[16] G. Herzberg, *Infrared and Raman Spectra* (Van Nostrand, New York, 1945).
[17] R. L. Shoemaker, S. Stenholm, and R. G. Berwer, Phys. Rev. A **10**, 2037 (1974).
[18] J. W. C. Johns, A. R. W. McKellar, T. Oka, and M. Römheld, J. Chem. Phys. **62**, 1488 (1975).
[19] W. H. Weber and R. W. Terhune, J. Chem. Phys. **78**, 6422 (1983).
[20] E. D. Hinkley, K. W. Nill, and F. A. Blum, *Infrared Spectroscopy With Tunable Lasers*, edited by H. Walther (Springer, Berlin, 1976), Vol. 2, p. 125.
[21] T. Shimizu, F. O. Shimizu, R. Turner, and T. Oka, J. Chem. Phys. **55**, 2822 (1971).
[22] F. Shimizu, J. Chem. Phys. **52**, 3572 (1970).
[23] W. H. Weber (private communication).
[24] R. L. Legan, J. A. Roberts, E. A. Rinehart, and C. C. Lin, J. Chem. Phys. **43**, 4337 (1965).
[25] V. S. Letokhov and V. P. Chebotayev, *Nonlinear Laser Spectroscopy* (Springer, Berlin, 1977), p. 255.